NONLINEAR OPTICS

Nonlinear optics refers to the alteration of the optical properties of a material by light (Boyd 2003). As light propagates through a material, it generates oscillating dipoles, which in turn give rise to electromagnetic radiation, allowing the light to continue. This process is typically described by the following simple relation:

$$P = \chi E$$

,

where P is the polarization of the material (dipole moment per unit volume), χ is a constant called the susceptibility, and E is the electrical field generated by the incident light. However, this linear relationship between polarization and electric field is a first order approximation to a more complicated functional relationship, which is better approximated by the higher order terms in the Taylor series expansion:

$$P = \chi^{(1)} \otimes E + \chi^{(2)} \otimes E^2 + \cdots$$

where $\chi^{(n)}$ refers the n-th order nonlinear susceptibility. Assuming that the magnitude of this constant, $\chi^{(n)}$, decreases with n, it becomes clear why we see second harmonic generation only in very strong electric fields. Applying a perturbation approach leads to the following approximation for the ratio of $\chi^{(n)}$ to $\chi^{(1)}$ as a function of electric field strength:

$$\frac{\chi^{(n)}}{\chi^{(1)}} \propto \left(\frac{E}{E_{atom}}\right)^{n-1}$$

1

As we will describe shortly, the second order polarization gives rise to the phenomenon of second harmonic generation. Therefore we calculate this fraction for $\chi^{(2)}$ for a mode-locked Ti-sapphire laser with an average power of 400 mW emitting 100 femtosecond pulses at a rate of 80 MHz. The power in a single pulse is then equal to the average power over a second divided by the fraction of time spent in pulses:

$$\text{Fraction of time pulsing} = \frac{8 \times 10^7 \text{ pulses}}{\text{second}} \frac{1 \times 10^{-13} \text{ seconds}}{\text{pulse}} = 8{\times}10^{-6}$$

$$\text{Power during pulse} = \frac{0.4W}{8 \times 10^6} = 5 \times 10^4 W$$

In order to determine the intensity of light from the incoming laser, we must also know the size of the beam at the focus. We will ignore the issues involved in the laser having a Gaussian intensity profile and approximate it as a collimated beam with a diameter of 4 mm. Following Mansuripur 1998, we take the size of the spot at the focus as the wavelength of light (800nm) divided by the numerical aperture. The numerical aperture of an ordinary glass lens is simply the index of refraction (which we take to be 1.6) multiplied by the sine of the angle between the edge of the beam and the focal point. Using a lens with a focal length of 38 mm, we calculate that the size of the spot will be 13 micrometers in diameter. The intensity at the focal point is then

$$Intensity = \frac{power}{area} = \frac{5 \times 10^4 W}{\pi \times (13 \times 10^{-6},)^2} = 9.4 \times 10^{13} W/m^2$$

which is approximately 1000 times smaller than the atomic electric field, so that each successive $\chi^{(n)}$ will be 1000 times smaller than the one before it. From this calculation, we can see the importance of maximizing the intensity of incident light during the pulses if we are to generate an appreciable second order polarization, $P^{(2)} = \chi^{(2)} E^2$

Second harmonic generation

As a wave propagating in space, E has the form (Hecht 2001) $E = E_0 \sin(\omega t)$, the polarization therefore has the form $P = \chi^{(1)} E_0 \sin(\omega t) + \chi^{(2)} E_0^2 \sin^2(\omega t) + \cdots$. However, since we know from trigonometry that $\sin^2(\omega t) = \frac{1 - \cos(2\omega t)}{2}$, the second order polarization bcomes

$$P^{(2)} = \frac{\chi^{(2)} E_0^2}{2}(1 - \cos(2\omega t))$$

To rephrase this result in English, we have an electric dipole being induced in the medium at double the frequency (half the wavelength) of the incoming laser light. This is similar to the technique of two-photon fluorescence in which two photons collide with a fluorophore in a narrow window of time, causing it to become excited and to emit a photon of light at slightly less than double the frequency of the incoming photons. Two-photon fluorescence and second harmonic generation are depicted schematically in Figure 1

.

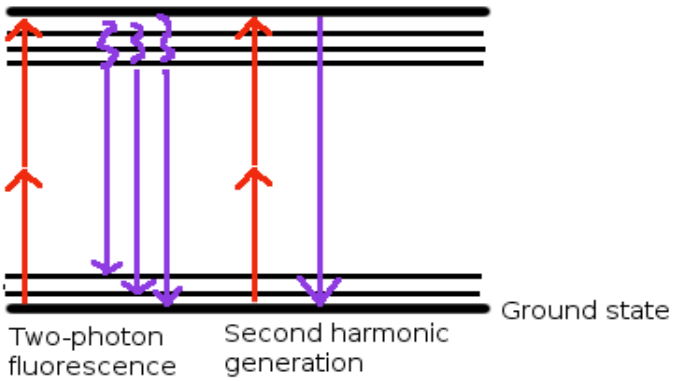

Figure 1 - Two-photon fluorescence versus second harmonic generation, Jablonski diagram

Although these two techniques are superficially similar, they arise from very different physical processes - two-photon fluorescence requires a fluorophore, which relaxes from the excited state through vibrational states before emitting a photon in a random direction. In contrast, second harmonic generation does not include relaxation through vibrational states, so no energy is lost to heat, a significant problem in temperature-sensitive biological tissues. Furthermore, second-harmonic generation produces a coherent beam of light in the forward direction only. Since it does not rely on excitation of a larger fluorophore, it is also much faster, and ought not to be as susceptible to photobleaching.

There are, however, certain strict conditions on the generation of second harmonics. The first is that only noncentrosymmetric objects can generate second harmonics, because the second-order nonlinear susceptibility $\chi^{(2)}$ is a vector average over the hyperpolarizability of the medium, which cancels out when the hyperpolarizability is the same in all directions.

The second condition is that of phase matching - in order to avoid destructive interference between second harmonics generated at different positions in the medium, which depletes an already weak signal, the original wavelength and the halved second harmonic wavelength can be made to propagate at the same speed. This is achieved despite the normal variation of the index of refraction with wavelength (e.g. prisms) by means of a birefringent crystal, which is a crystal with different indices of refraction at different polarization angles. For example, for a crystal which propagates light more slowly at lower wavelengths and more slowly on the ordinary axis of the crystal (negative uniaxial crystal), it is possible to achieve this at a tunable angle of the crystal relative to the polarized light of the laser, ensuring constructive interference in the forward direction.

Experimental Setup

Second harmonic generation begins with a mode-locked Ti:Sapphire laser, the set-up of which is beyond the scope of this paper. Using a glass slide, we divert approximately 4% of the laser beam to a spectrometer that is used to measure the spectrum of the emitted light. When the laser is mode-locked, the spectrum is broad, usually spanning the wavelengths 770-790 nm. Passing through the glass slide, the rest of the beam is directed to the optical axis by a set of mirrors. Using two flipping-mirrors (c and d in Figure 2), we are able to create two paths to the optic axis. When mirror c is down and d is up, there is a static path that can be used for aligning elements of the optic axis and checking on the generation of the second harmonics. Switching the status of the mirrors directs the light path to a set of scanning mirrors (e), which are controlled via a laptop running Matlab and connected to a data acquisition card.

The beam next passes through a beam expander. We used a telescope system with a -25.4 mm lens and a 75.6 mm lens, expanding the beam by approximately 3 times. The goal of the beam expander is to get the beam to fill the back of the objective. The 3x expansion made our beam approximately 6 mm in diameter.

After the expander, the beam passes through a wave plate and polarizing beam splitter. The wave plate adjusts the polarization of the light, and the beam splitter diverts light of a particular polarization away while letting the remaining light through. The wave plate and polarizing beam splitter, then, work together to serve as an attenuator for the beam. Rotating the wave plate allows different amounts of light to pass through the beam splitter. This is important, as we found that at full power the laser could burn biological tissue if left in one place.

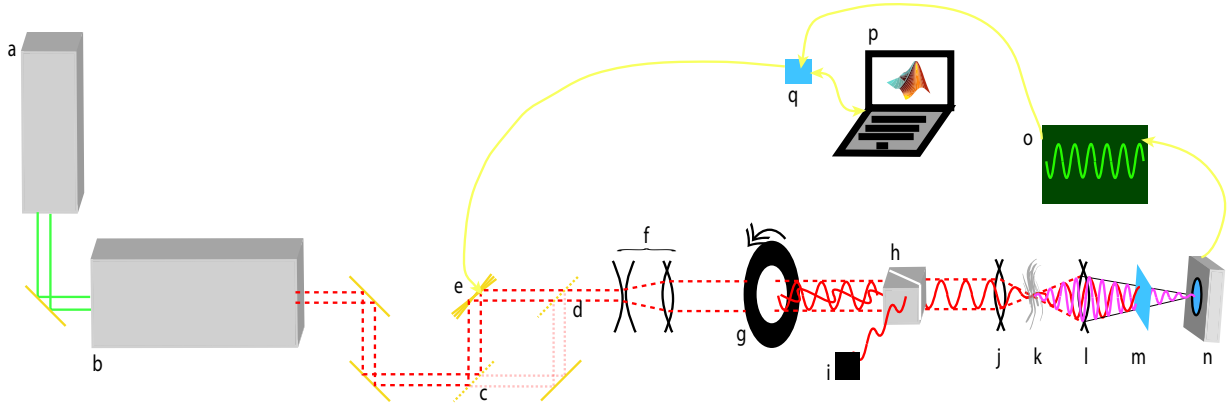

Figure 2: Experimental Setup. The setup is described in the text.
a. Pumping laser. b. Ti:Sapphire Laser. c,d. Flipping mirrors. e. Scanning mirrors. f. Beam expander. g. Rotating wave plate. h. Polarizing beam splitter. i. Beam block for beam deflected from h. j. Objective lens. k. Sample. l. Collecting lens. m. Blue filter. n. Photodiode. o. Oscilloscope. p. Laptop. q. Data acquisition card.

An objective or lens is used to collect the remaining light and focus it onto the sample. We used a 38.1 mm lens. For our sample, we began with BBO crystal. We also tried to generate harmonics from a piece of bone and from a section of tendon from a rat tail. Unfortunately, only the BBO crystal was successful in producing second harmonics. Successful second harmonic generation produces a violet light. Because most photons do not get converted by second harmonic generation, a strong red beam will also come through. A blue filter blocks this beam.

We used a 25.4 mm collecting lens to focus the beam onto a photo diode. By attaching a narrow band-pass filter to the photo diode and adjusting the wavelength of the mode-locked laser, we were able to determine that the light being generated was second-harmonic light, not auto-fluorescence of the sample. The photo-diode was connected to an oscilloscope, and the magnitude of the signal was recorded using the laptop and data acquisition card.

We were successful in generating a second harmonic signal from BBO crystal, however we were not able to record a signal from biological tissue as we had originally hoped. Here are some ideas for making this successful in the future. First, make sure the mirrors used will reflect almost all the light with wavelength 750-800 nm. This is especially important to keep in mind when selecting a set of scanning mirrors: the first set we tried transmitted the majority of the light. We also had our pumping laser at a 90° angle to the Ti:Sapphire laser. A representative of the Tsunami Laser Company told us that this was bad practice and beam from the pumping laser should go directly into the second laser. It is possible that this would make the Ti:Sapphire laser easier to get into mode lock.

We chose to use a 38.1 mm lens in place of a traditional objective in our setup. This worked well for the BBO crystal, but may have lost too much power for other samples. The goal of the beam expander is to cover the back aperture of the objective. Because we used a lens, we may have needed a larger expansion. On the other hand, the back of an objective is generally smaller than 6 mm, so a smaller expansion should be used.

We used only one photo diode to collect the second harmonic light, and we found that our eyes were more sensitive than the photo diode. That is, we could see a clear signal even when the oscilloscope reading was indistinguishable from its reading when the beam was blocked entirely. That we never a saw second harmonic signal from the tendon may not mean that no signal was generated. We had hoped to be able to use the photodiode and oscilloscope to detect signals that were not visible to our eyes. With one photodiode this is not possible. Two potential solutions come to mind.

First, it would be helpful to collect the portion of the signal that is back propagated from the sample. This may be achieved by inserting a dichroic mirror between the beam splitter and the objective lens. The dichroic mirror should transmit light in the range of the red beam and reflect light in the range of the violet beam. The reflected light from this mirror could then be collected by a second photodiode, and the signal added to that of the first. Another potentially useful solution would be to try using photo multiplier tubes instead of photodiodes; these should be more sensitive than the human eye.

RESULTS

Although we were unable to generate second harmonics in tendon, as desired, we were able to generate them from BBO crystal, and could explore some properties of this signal.

First, we showed that the second harmonic signal in BBO crystal is strongly dependent on the rotation of the crystal. The amount of second harmonic signal depends on the degree of phase-matching between the red and violet light. As the crystal is rotated, the angle, theta, between the ordinary axis of the crystal and polarization of the light varies, which varies the index of refraction for the 400 nm light. Thus, the degree of phase-matching between the two wavelengths varies with the angle of the crystal, so the strength of the signal should vary as well.

Results are shown in Figure 3. The blue line shows our first set of measurements. We expect the results to be periodic, with period some factor of 360°. We began measuring at 160°, which is where we had found maximal signal strength. We were surprised that when we had rotated the crystal 360°, our signal had diminished from 32 μW to 6 μW. To check our measurements, we repeated the experiment, rotating 45° at a time. Results, plotted as green dots, show the same pattern.

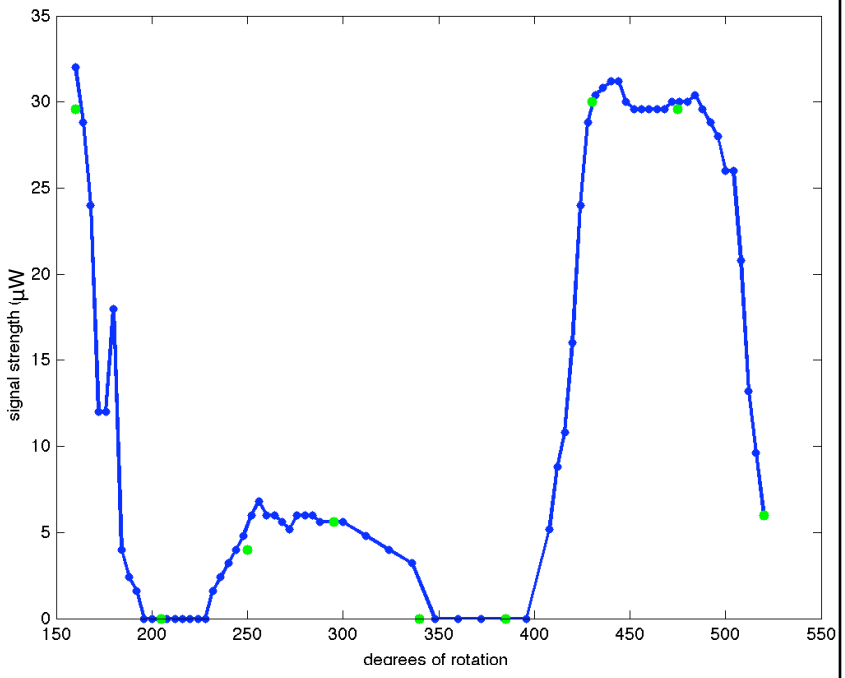

Figure 3. Strength of second harmonic signal is dependent on the rotation of the crystal, but may be sensitive to yet undetermined properties of the laser.

Looking at the pattern of results, it appears that there are three levels at which the signal may plateau: no signal (0-1.5 μW)[1], weak signal (5-8 μW), and strong signal (28-32 μW). Between these plateaus are fairly sharp transitions.

We hypothesize that the plateaus are relatively stable, but the location of the transition could be sensitive to parameters of the laser. In particular, notice that the first sharp descent is "interrupted" briefly, but if the first five measurements were shifted by 20°, the curve would be smooth and monotonic. Similarly, the descent at the end would line up nicely

[1] Note that the signal never disappeared completely to our eyes. The signal on the oscilloscope, however, was indistinguishable from a blocked beam when it reached 1.3 mW. All such values are plotted as 0 on the graph.

with the descent at the beginning if we imagined this as having a period of 330°.

It is not clear what is causing the instability in where the transitions occur. We monitored the input power carefully during this experiment; all measurements were made with the mode-locked laser at a power of 420-430 mW. We often noticed a seeming "bistability" in the oscilloscope signal that would persist for a moment when we turned the crystal. That is, for a moment the oscilloscope would vacillate between two different amplitudes. This usually resolved itself quickly and we took the data point once it settled. We found that, in general, the mode-locking of the laser was unstable, and we suspect this instability could have contributed to the bistable oscilloscope signal and to the instability in where the transitions between strong and very weak signals occurred.

For our next experiment, we set the crystal at a rotation of 200° (at the time, this was the strongest signal point) and then measured the power of the input laser and the output second harmonic signal as we rotated the wave plate. This data (see figure 4) shows a robust periodic effect with period of 90°. This shows, first, that the wave plate, indeed, attenuates the power of the mode-locked laser, as predicted.

The periodicity of the second harmonic response also demonstrates that the dependence on the input intensity of the second harmonic signal is robust. Finally, we can see that the input intensity varies between 15 and 350 mW, while the second harmonic signal varies between 0 and 30 μW.

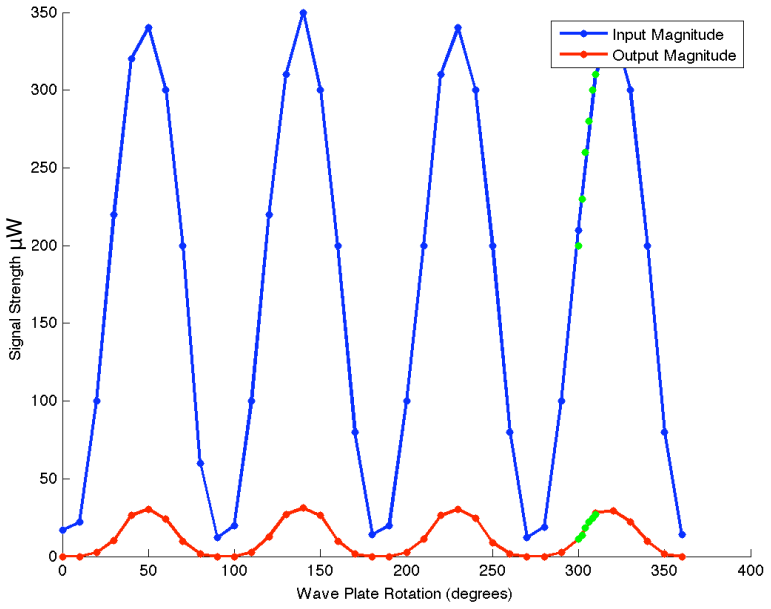

Figure 4. Rotating the wave plate causes a robust, periodic effect on the amplitude of each signal. Note that the input signal is several orders of magnitude greater than the output.

Theoretical calculations, $P = \chi^{(1)} \otimes E + \chi^{(2)} \otimes E^2 + \cdots$, suggest that the strength of the second harmonic signal will vary with the intensity of the input signal, squared. To test this, we plotted the input intensity vs. output intensity and fitted the data with a quadratic function (see Figure 5). Looking at a log-log plot of the same data reveals the quadratic relationship between input intensity and second harmonic generation. The least-squares fit for the log-transformed data is y = 1.968x - 8.081, with an r-squared value of .987. The 95% confidence interval for the slope is (1.877, 2.059), so 2 is included. We conclude that there is good evidence that the output intensity does vary quadratically with input intensity.

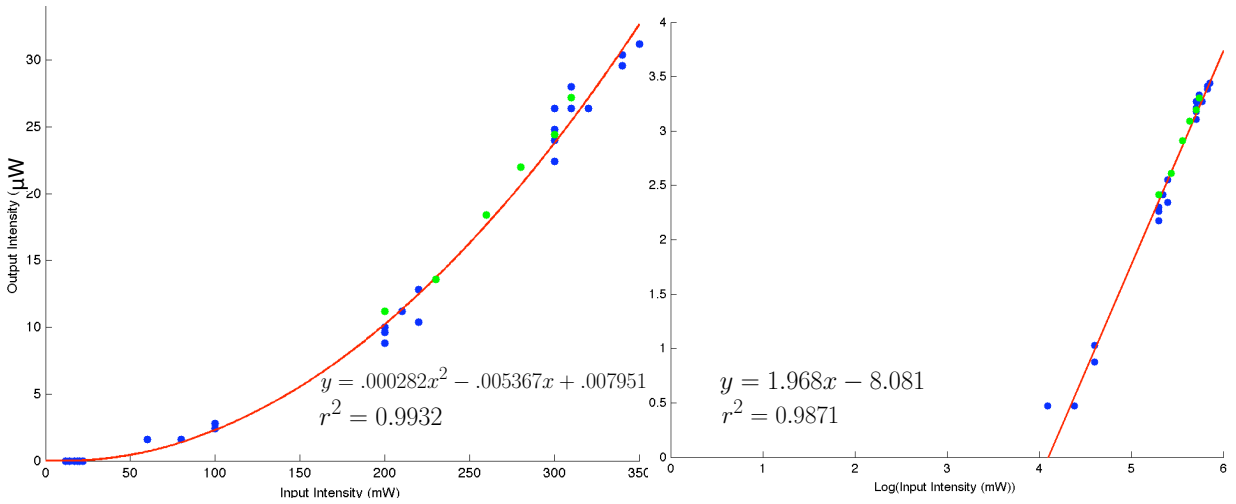

Figure 5. Input intensity vs. output intensity (regular and log-log plots). Blue dots were taken from measurements made every 10 degrees of wave plate rotation and were used for curve-fitting. Red curves are best fits, calculated with the Matlab curve fitting toolbox. Green dots were taken every 2 degrees of rotation between 300 and 310 degrees. They were not used in determining best fit, but appear to lie along the best fit curve. The figures show that the intensity of the second harmonic signal varies quadratically with the intensity of the incoming beam.

Conclusion

We have generated second harmonics by collimating and then focusing a mode-locked Ti-sapphire laser onto a birefringent crystal. We obtained experimental verification of several important features of second harmonic generation: namely, that the strength of the light varies quadratically as a function of the intensity of the incident beam, and that the polarization of the incident light relative to the ordinary axis of the birefringent crystal determines the strength of the second harmonic, in keeping with theoretical predictions based on phase matching. We furthermore showed that the light generated was at precisely half the wavelength by means of a narrow band filter, and we were able to generate second harmonics in a scanning configuration.

It is our hope that future students will be able to build upon these results by imaging the collagen fibrils in a rat tail, replicating published results from Freund et al (1986). Although we were successful in exploring some of the fundamental physical aspects of nonlinear optics with this project, we were not successful in our ultimate goal of applying this tool to neurobiology. With the scanning configuration in place, it ought to be possible to study the polarity of filaments in cells, including the microtubules in neuronal processes (Kwan et al 2008). The use of styryl dyes to optically record action potentials in neurons using second harmonic generation offers the possibility of a fast readout of neural activity that could penetrate deeply into tissue without the sort of heating encountered in traditional two-photon microscopy (Helmchen and Denk 2006). This might not be beyond future generations of students in this Biophysics course.

Bibliography

1. Freund, I., Deutsch, M. & Sprecher, A. Connective tissue polarity. Optical second-harmonic microscopy, crossed-beam summation, and small-angle scattering in rat-tail tendon. Biophysical Journal 50, 693-712(1986).
2. Helmchen, F. & Denk, W. Deep tissue two-photon microscopy. Nat. Methods 2, 932-940(2005).
3. Boyd, R.W. Nonlinear optics. 578(Academic press: 2002).
4. Dombeck, D.A., Blanchard-Desce, M. & Webb, W.W. Optical Recording of Action Potentials with Second-Harmonic Generation Microscopy. J. Neurosci. 24, 999-1003(2004).
5. Hecht, E. Optics. 680(Pearson Education, Limited: 2001).
6. Kwan, A.C., Dombeck, D.A. & Webb, W.W. Polarized microtubule arrays in apical dendrites and axons. Proceedings of the National Academy of Sciences 105, 11370-11375(2008).
7. Campagnola, P.J. & Loew, L.M. Second-harmonic imaging microscopy for visualizing biomolecular arrays in cells, tissues and organisms. Nat Biotech 21, 1356-1360(2003).
8. Mansuripur, M. The Physical Principles of Magneto-Optical Recording. 776(Cambridge University Press: 1998).